Progress In Electromagnetics Research, Vol. 114, 429–441, 2011

SUBWAVELENGTH ARRAY OF PLANAR TRIANGLE MONOPOLES WITH CROSS SLOTS BASED ON FAR-FIELD TIME REVERSAL

G.-D. Ge, D. Wang, and B.-Z. Wang †

Institute of Applied Physics
University of Electronic Science and Technology of China
Chengdu 610054, China

Abstract—A subwavelength array of planar triangle monopole antennas is proposed and discussed in this paper. Each element of the array is etched with many cross slots which bring no effects to the element's performances of voltage standing wave ratio and far-field radiation patterns. An important property of this antenna is that if multiple such planar antennas are placed face to face, the proposed array can perform time-reversal far-field focusing with a super-resolution as small as one twentieth of a wavelength. The proposed subwavelength array is easy to design and convenient for integration.

1. INTRODUCTION

Antenna system has wide applications in mobile electronics such as wireless mobile communication, radio frequency identification (RFID), and wireless sensor network [1–13]. These systems, aiming to achieve multiple-antenna design with multiple independent channels on size-limited platforms, always seek means to greatly improve the capacity and data-rate of communication. According to traditional antenna theory, in order to obtain excellent gain of space diversity and space multipexing, the minimum distance between antenna units should be more than one half-wavelength, thus causes large physical volume in structure. Moreover, the diffraction limit of electromagnetic wave due to the loss of evanescent waves in the far field which carry high spatialspectrum information, restrains the resolution of

Received 17 February 2011, Accepted 9 March 2011, Scheduled 10 March 2011
Corresponding author: Guang-Ding Ge (geguangding@uestc.edu.cn).
† G.-D. Ge is also with College of Electronic and Information Engineering, Nanjing University of Information Science and Technology, Nanjing 210044, China.

electromagnetic devices. Despite many efforts are put for minimization of antenna units, integration of multiple antennas with independent channels on size-limited mobile electronic terminals is still a challenge. Therefore, the conception of subwavelength antenna system, which could achieve reduction of device space with electromagnetic time reversal (TR) technique, leads to one new research direction for compact wireless mobile terminals.

Featuring of its adaptive focusing characteristic, TR technique has been used in lots of applications such as underwater acoustics communication, medical, electromagnetic imaging, and ultra-wideband wireless communication [1–19]. Recently, one completely new approach to achieve super-resolution has been offered by TR technique [20–22]. In 2007, a subwavelength array with a distance of $\lambda/30$ between each antenna element was proposed to exploit the far-field super-resolution characteristics of TR electromagnetic wave for high-quality communication in a reverberant chamber [23–26]. Based on these researches, we have recently done several simulations and experiments about TR electromagnetic wave [27–30], as well as further researches for super-resolution by combining TR with subwavelength array [31]. In particularly, as pointed out in [32] that in the subwavelength array, each antenna element could hold independent high-data-rate communication at 500 Mb/s when distance between each element is $\lambda/15$. This result offers important inspiration for the simplification of subwavelength array structure.

In this paper, a compact subwavelength array of planar triangle monopole antennas is proposed. Each triangle monopole antenna is etched with many microstructured cross slot, and different locations of the cross slots lead to three different kinds of antenna as shown in Figure 1. Through comparison of the electromagnetic characteristic of these antenna elements, and the resolution characteristic of their corresponding arrays, we find the subwavelength array with ideal super-resolution.

2. EXPERIMENTS AND ANALYSIS

2.1. Performance of Individual Planar Monopole

Three different types of antenna elements are depicted in Figure 1(a), Figure 1(b), and Figure 1(c), respectively These antennas are all built on the 36 mm × 90 mm × 0.5 mm substrates with a relative permittivity of $\varepsilon_r = 2.2$. The input impedance of the feeding line is 50 Ω and 14.1 mm long. The impedance matching lines, L_1 and L_2, are both 16.0 mm long. For the radiation part, the base line W_3 is 30 mm and the height H_3 is 39.5 mm. All microstructured cross slots etched on perfect

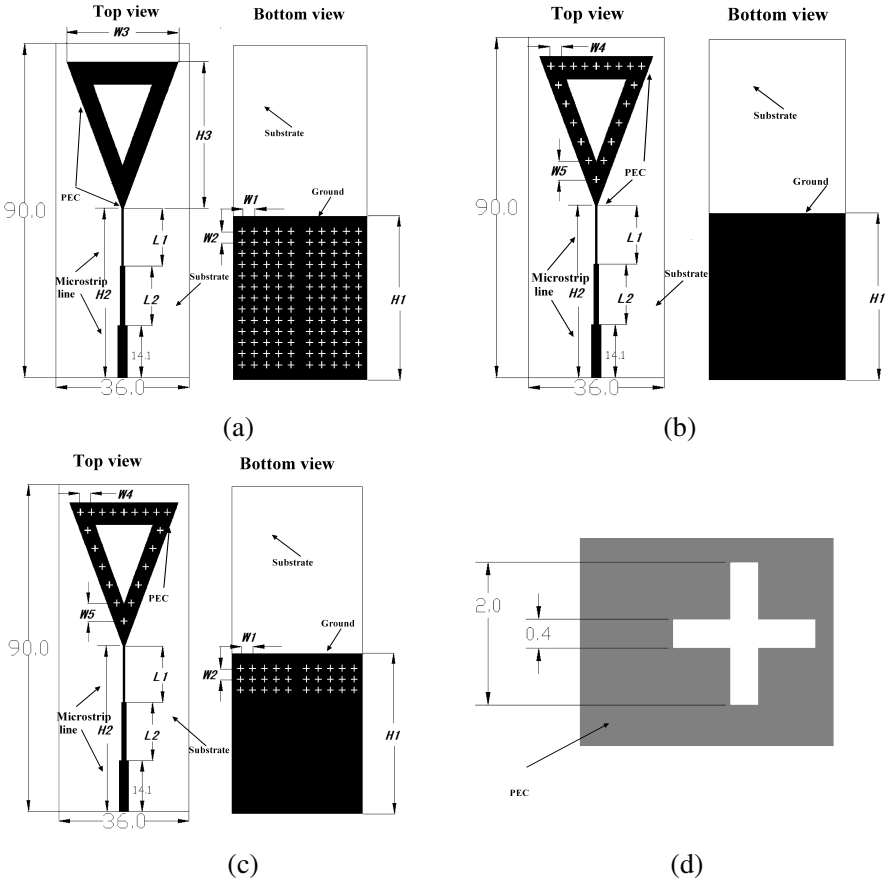

Figure 1. Details of three antenna elements, (a) cross slots etched on the ground floor of the feeding line, (b) cross slots etched on the radiation part, (c) cross slots etched on both the radiation part and the ground floor of the feeding line, and (d) the cross slot. (units: mm).

electric conductor (PEC), and the dimension of the cross slot is shown in Figure 1(d). The arrangement of the first type antenna is presented in Figure 1(a), where the cross slots are not etched on the triangle radiation part, but only on the ground floor of the feeding line, and the distance W_1 between the slots in the horizontal direction is 3.3 mm, W_2 in the vertical direction is 3.0 mm. Arrangement for the second type antenna is shown in Figure 1(b), where the cross slots are only etched on the triangle radiation part with W_4 in the horizontal direction being 3.0 mm and W_5 in the vertical direction 5.0 mm, and the feeding line

has an ordinary ground floor. Figure 1(c) is for the last type antenna element, where the cross slots are etched on both the triangle radiation part and the ground floor of feeding line, and the cross slots on the floor, in a different way from Figure 1(a), are only etched at the upper edge near the triangle radiation element with three rows of the cross slots. Simulation results of VSWRs and radiation patterns for the three type antennas are all given in Figure 2 and Figure 3. In the frequency range

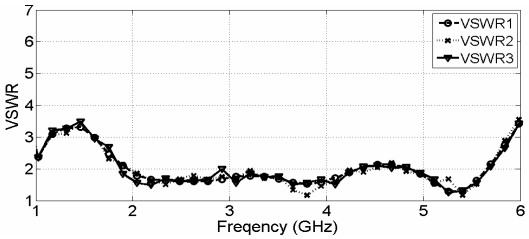

Figure 2. Simulation results of VSWRs of the antennas in Figure 1, VSWR1 for the antenna in Figure 1(a), VSWR2 for Figure 1(b), and VSWR3 for Figure 1(c).

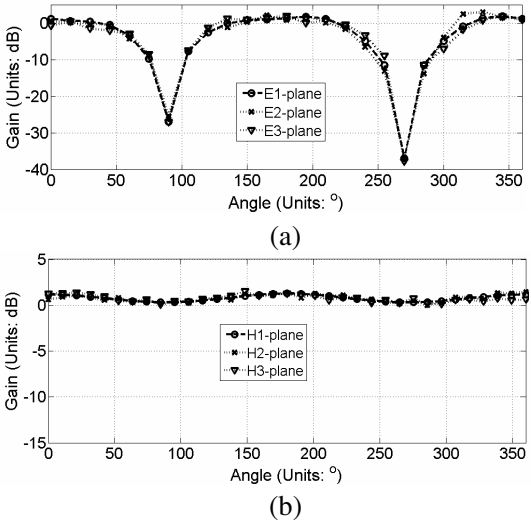

Figure 3. Simulation results of far-field radiation patterns of the antennas in Figure 1 at 3.5 GHz. (a) E-plane copolarization patterns, E_1-plane for the antenna in Figure 1(a), E_2-plane for Figure 1(b), and E_3-plane for Figure 1(c). (b) H-plane copolarization patterns, H_1-plane for the antenna in Figure 1(a), H_2-plane for Figure 1(b), and H_3-plane for Figure 1(c).

from 2.4 GHz to 5.5 GHz, these three curves for VSWR, all smaller than 2.2, are almost the same. When it comes to the radiation patterns, the clear comparison is given Figure 3(a) and Figure 3(b). In Figure 3(a), under the test frequency 3.5 GHz, E_1-plane, E_2-plane and E_3-plane, are the E-plane copolarization radiation patterns. And in Figure 3(b), under the test frequency 3.5 GHz, H_1-plane, H_2-plane and H_3-plane, are the H-plane copolarization radiation patterns. Comparison of the results demonstrates that the radiation characteristics for these three type antenna elements witness no great difference. Based on these simulation results, it shows that these three antenna elements exhibit relatively stable and similar radiation characteristics in the whole frequency range, so the cross slots structures would not cause change to the performance of combination antenna element.

2.2. Super-resolution Characteristics of Subwavelength Array

When four such etched planar monopoles in Figure 1(c) are placed face to face at an interval of $\lambda/20$ apart from one another along the z direction, shown as in Figure 4, they form a subwavelength array, where λ is the wavelength of the centre operation frequency. This array can display far-field super-resolution characteristics in a time-reversal electromagnetic wave system.

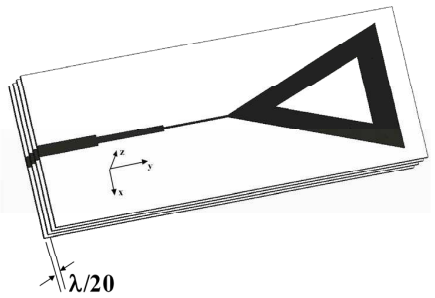

Figure 4. Proposed subwavelength array with four planar triangle monopoles.

In literature [23] and [32], the mechanism of far-field super-resolution characteristic for TR electromagnetic wave are concluded as follows: the fine subwavelength information in the near-field evanescent waves are converted into the far-field propagating waves with the aid of randomly-distributed metal wires around each array element. Here, through the aperiodical cross slots on each planar triangle monopole,

near-field evanescent waves can be converted into propagating waves which can be received, time-reversed by a time reversal mirror (TRM) in the far-field, and then re-transmitted back. Based on [33] and [34], evanescent waves and propagating waves are reciprocal, so the far-field time-reversed wave generated from the evanescent waves of the source is converted back into initial evanescent components, which therefore plays important roles for super-resolution refocusing. In order to verify the working mechanism, experiments have been conducted as follows.

As shown in Figure 5, the proposed subwavelength array are tested in an electromagnetic TR experiment system. The subwavelength array is 40λ away from a TRM which is made up of two identical bowtie antennas with ultra wideband property and simple structure [35]. One modulated Gaussian pulse signal with a spectrum range of 2.4 GHz–5.5 GHz is transmitted by an Arbitrary Waveform Generator AWG7122B from Tektronix, and received by a Digital Serial Analyzer DSA72004B from Tektronix.

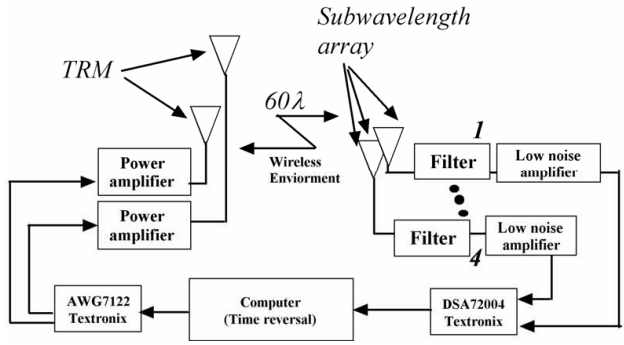

Figure 5. Electromagnetic TR experiment system for the proposed subwavelength array.

The whole experiment is divided into three steps:

Firstly, original pulse $x(t)$ is transmitted from the first antenna in the TRM for channel sounding. After transmission, signal received at the nth ($n = 1, 2, \ldots, 4.$) element in the subwavelength array is recorded as $y_{1,n}(t)$. Then, $x(t)$ is transmitted again from the second antenna in the TRM and the received signals at the subwavelength array are recorded as $y_{2,n}(t)$ ($n = 1, 2, \ldots, 4.$). Due to reciprocity of the channels, $y_{m,n}(t)$ ($m = 1, 2$) also represents the received signal at the mth antenna in the TRM when $x(t)$ is transmitted from the nth element in the subwavelength array.

Secondly, $y_{m,n}(t)$ ($n = 1, 2, \ldots, 4.$) is time-reversed to $y_{m,n}(-t)$ based on the first-in-last-out rule. Then $y_{1,n}(-t)$ and $y_{2,n}(-t)$ are

transmitted simultaneously from the first and second antennas in the TRM, and the final signals would be received at the ith element in the subwavelength array, denoted as $y_{i,n}^{TR}(t)$ $(i = 1, 2, \ldots, 4.)$.

Thirdly, we record the peak values $A_{i,n}$ of signal $y_{i,n}^{TR}(t)$ $(i = 1, 2, \ldots, 4.)$ and observe the super-resolution characteristics of the array.

In the experiment, subwavelength array in Figure 4 is constructed with the monopole shown in Figure 1(c), and the original signal $x(t)$ for transmission is depicted in Figure 6. The signals received at the TRM, $y_{1,2}(t)$ and $y_{2,2}(t)$, sent from the second element of the subwavelength array, are given in Figures 7(a)–(b). The final signals $y_{i,2}^{TR}(t)$ $(i = 1, 2, \ldots, 4.)$ received at the four etched planar triangle monopoles after time reversal and re-transmission are demonstrated in Figures 8(a)–(d). Furthermore, the peak values $A_{i,2}$ of signals $y_{i,2}^{TR}(t)$ $(i = 1, 2, \ldots, 4.)$ are normalized to $A_{2,2}$ and then depicted as curve 'Antenna-2' in Figure 9. As shown in this curve, $A_{i,2}$ $(i = 1, 3,$ and $4)$ are smaller than half of $A_{2,2}$, which means that signals are mainly focusing back at the second antenna element in this subwavelength array. Super-resolution characteristics are observed

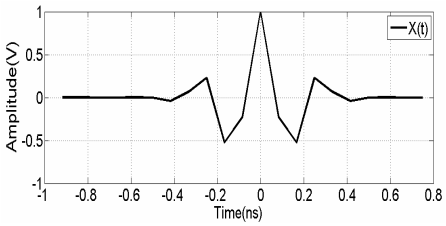

Figure 6. The original signal $x(t)$.

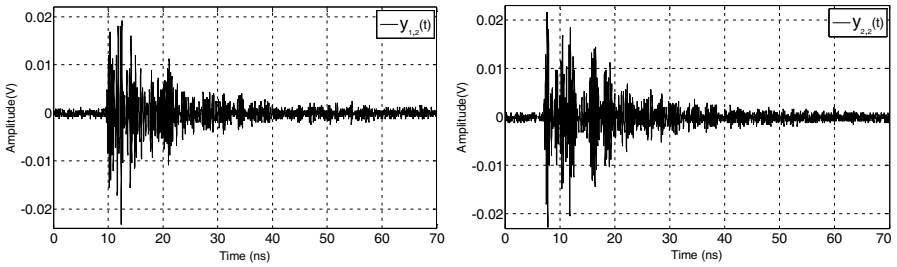

Figure 7. Received signals at the TRM, (a) $y_{1,2}(t)$ and (b) $y_{2,2}(t)$, sent from the second element of the subwavelength array.

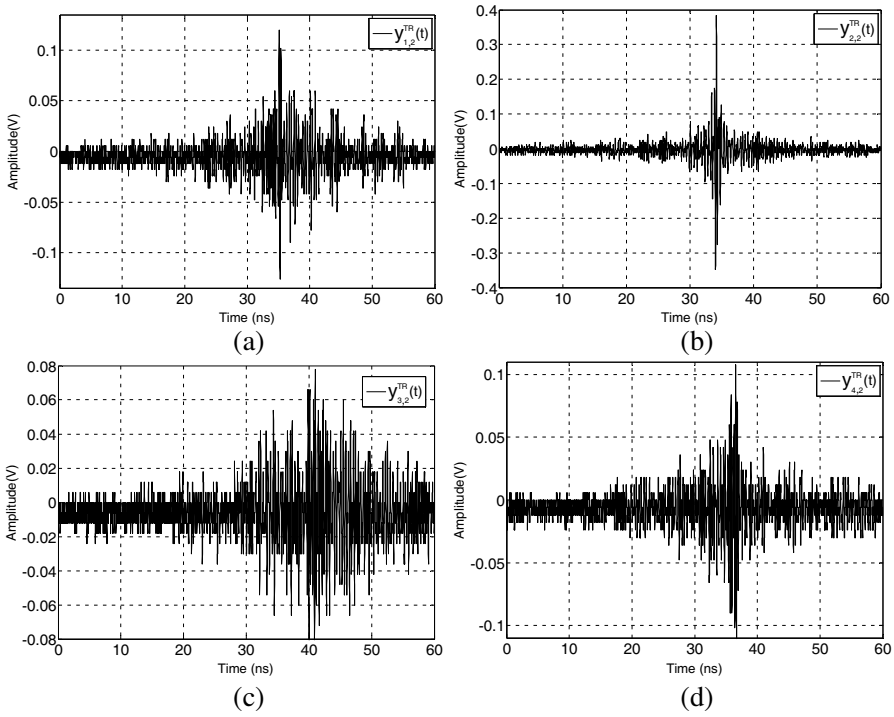

Figure 8. The final signals $y_{i,2}^{TR}(t)$ $(i = 1, 2, \ldots, 4.)$ received at the four etched planar triangle monopoles after time reversal and retransmission. (a) $y_{1,2}^{TR}(t)$, (b) $y_{2,2}^{TR}(t)$, (c) $y_{3,2}^{TR}(t)$, and (d) $y_{4,2}^{TR}(t)$.

from curve 'Antenna-2' as expected. For $n = 1$, 3, and 4, we can similarly get other curves 'Antenna-1', 'Antenna-3', and 'Antenna-4' shown as in Figure 9 and observe the super-resolution characteristics.

Curves in Figure 9 prove that the array constructed with the monopole in Figure 1(c) really has super-resolution focusing characteristic. Nevertheless, if we take the monopoles in Figure 1(a) and Figure 1(b) as the element to build up one 4-element array as well, and follow the same steps as above, we can get the results in Figure 10 and Figure 11. Viewing from the results of the other two arrays, we can find that if the cross slots are only etched on the triangle radiation part or the ground floor of the feeding line, neither of the arrays can demonstrate ideal super-resolution focusing. Actually, if the triangle radiation part was not etched with cross slots, evanescent waves near the antenna element would have failed to be transformed into propagating waves after the TR operation, thus the super-resolution

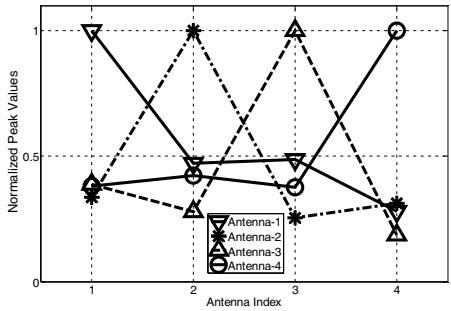

Figure 9. Experiment results for the normalized peak values of the received TR signals at the four elements of the subwavelength array constructed with the monopole shown in Figure 1(c). It demonstrates the super-resolution focusing characteristics of the array. Curves "Antenna-1", "Antenna-2", "Antenna-3", and "Antenna-4" stand for the normalized peak values of signals, $A_{i,1}$ ($i = 1$, 2, 3, and 4), $A_{i,2}$, $A_{i,3}$, and $A_{i,4}$, respectively.

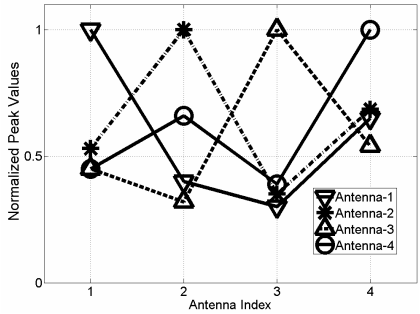

Figure 10. Experiment results for the normalized peak values of the received TR signals at the four elements of the subwavelength array constructed with the monopole shown in Figure 1(a). Curves "Antenna-1", "Antenna-2", "Antenna-3", and "Antenna-4" stand for the normalized peak values of signals, $A_{i,1}$ ($i = 1, 2, 3,$ and 4), $A_{i,2}$, $A_{i,3}$, and $A_{i,4}$, respectively.

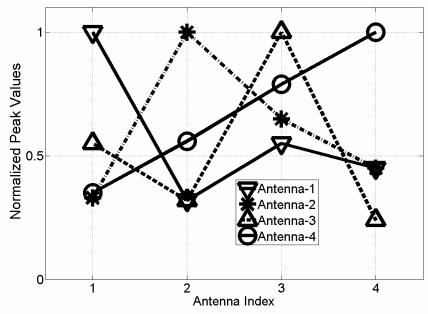

Figure 11. Experiment results for the normalized peak values of the received TR signals at the four elements of the subwavelength array constructed with the monopole shown in Figure 1(b). Curves "Antenna-1", "Antenna-2", "Antenna-3", and "Antenna-4" stand for the normalized peak values of signals, $A_{i,1}$ ($i = 1, 2, 3,$ and 4), $A_{i,2}$, $A_{i,3}$, and $A_{i,4}$, respectively.

characteristics would not have been achieved. Additionally, since the upper edge of the ground floor is also an essential radiation part of the monopole, if the floor was not etched with cross slots as shown in Figure 1(b), the subwavelength array would still obtained no super-resolution characteristics. Based on the above analysis, we choose the antenna element in Figure 1(c) to construct the subwavelength array, and get ideal super-resolution focusing characteristic with the aid of TR technique. When compared with the metal-wires array [23], the subwavelength array proposed in this paper, with the antenna element distance of only $\lambda/20$, achieves important improvement in structure simplification, and owns great convenience for fabrication and integration.

3. CONCLUSION

This paper proposes a subwavelength array of planar triangle monopoles with microstructured cross slots. Simulation results of far-field radiation pattern and VSWR show that the cross slot structures do not alter radiation performance of individual antenna element. An important property of this array is that it can perform time-reversal far-field focusing with a super-resolution as small as 1/20 wavelength. The subwavelength array with planar structures could lead to volume reduction for wireless terminals. And this subwavelength array, compared with the complicated random distribution of a big number of metal wires around the short monopoles [23], witnesses great simplification and thus gains significant advantage for easy integration.

ACKNOWLEDGMENT

This work was supported by the High-Tech Research and Development Program of China (No. 2008AA01Z206), the Research Fund for the Doctoral Program of Higher Education of China (No. 20100185110021), the National Natural Science Foundation of China (No. 61071031), and Project 9140A01020110DZ0211.

REFERENCES

1. Bellomo, L., S. Pioch, M. Saillard, and E. Spano, "Time reversal experiments in the microwave range: Description of the radar and results," *Progress In Electromagnetics Research*, Vol. 104, 427–448, 2010.

2. Zhang, W., A. Hoorfar, and L. Li, "Through-the-wall target localization with time reversal music method," *Progress In Electromagnetics Research*, Vol. 106, 75–89, 2010.
3. Dmitriev, V., "Space-time reversal symmetry propensties of electromagnetic Green's tensors for complex and bianisotropic media," *Progress In Electromagnetics Research*, Vol. 48, 145–184, 2004.
4. De Cos, M. E., Y. Alvarez lopez, and F. Las-Heras, "Planar artificial magnetic conductor: Design and characterization setup in the RFID SHF band," *Journal of Electromagnetic Waves and Applications*, Vol. 23, No. 11–12, 1467–1478, 2009.
5. Jarchi, S., J. Rashed-Mohassel, and R. Faraji-Dana, "Analysis of microstrip dipole antennas on a layered metamaterial substrate," *Journal of Electromagnetic Waves and Applications*, Vol. 24, No. 5–6, 755–764, 2010.
6. Yang, C.-F., M. Cheung, C.-Y. Huang, and J.-S. Sun, "Print a compact single- and quad-band slot antenna on ceramic substrate," *Journal of Electromagnetic Waves and Applications*, Vol. 24, No. 13, 1697–1707, 2010.
7. Gurel, C. S. and E. Yazgan, "Resonant frequency of air gap tuned circular microstrip antenna with anisotropic substrate and superstrate layers," *Journal of Electromagnetic Waves and Applications*, Vol. 24, No. 13, 1731–1740, 2010.
8. Ling, J., S.-X. Gong, B. Lu, H.-W. Yuan, W.-T. Wang, and S. Liu, "A microstrip printed dipole antenna with UC-EBG ground for RCS reduction," *Journal of Electromagnetic Waves and Applications*, Vol. 23, No. 5–6, 607–616, 2009.
9. Yeo, J. and D. Kim, "Novel tapered AMC structures for backscattered RCS reduction," *Journal of Electromagnetic Waves and Applications*, Vol. 23, No. 5–6, 697–709, 2009.
10. De Cos, M. E., Y. Alvarez Lopez, and F. Las-Heras, "A novel approach for RCS reduction using a combination of artificial magnetic conductors," *Progress In Electromagnetics Research*, Vol. 107, 147–159, 2010.
11. Zhang, Y., B. Z. Wang, W. Shao, W. Yu, and R. Mittra, "Artificial ground planes for performance enhancement of microstrip antennas," *Journal of Electromagnetic Waves and Applications*, Vol. 25, No. 4, 597–606, 2011.
12. Wei, F., L. Chen, X.-W. Shi, Q.-Y. Wu, and Q.-L. Huang, "Design of compact UWB power divider with one narrow notch-band," *Journal of Electromagnetic Waves and Applications*, Vol. 24, No. 17–18, 2343–2352, 2010.

13. Xu, H.-Y., H. Zhang, X. Yin, and K. Lu, "Ultra-wideband Koch fractal antenna with low backscattering cross section," *Journal of Electromagnetic Waves and Applications*, Vol. 24, No. 17–18, 2615–72623, 2009.
14. Guo, N., B. M. Sadler, and R. C. Qiu, "Reduced-complexity UWB time-reversal techniques and experimental results," *IEEE Trans. Wireless Commun.* Vol. 6, No. 12, 4221–4226, Dec. 2007.
15. Lerosey, G., J. de Rosny, A. Tourin, A. Derode, G. Montaldo, and M. Fink, "Time reversal of electromagnetic waves," *Phys. Rev. Lett.*, Vol. 92, No. 19, 193904-1–3, May 2004.
16. Lerosey, G., J. de Rosny, A. Tourin, A. Derode, and M. Fink, "Time reversal of wideband microwaves," *Appl. Phys. Lett.*, Vol. 88, 154101-1–4, Apr. 2006.
17. Scott, I., A. Vukovic, and P. Sewell, "Krylov acceleration techniques for time-reversal design applications," *IEEE Trans. Microwave Theory Tech.*, Vol. 58, No. 4, 917–922, Apr. 2010.
18. Jin, Y., J. M. F. Moura, and N. O'donoughue, "Time-reversal in multipleinput multipleoutput radar," *IEEE J. Selected Topics in Signal Processing*, Vol. 4, No. 1, 210–225, Feb. 2010.
19. Jin, Y. and J. M. F. Moura, "Time-reversal detection using antenna array," *IEEE Trans. Signal Processing*, Vol. 57, No. 4, 1396–1414, Apr. 2009.
20. Song, H. C., W. S. Hodgkiss, W. A. Kuperman, T. Akal, and M. Stevenson, "Multiuser communications using passive time reversal," *IEEE Journal of Oceanic Engineering*, Vol. 32, No. 4, 915–922, Oct. 2007.
21. De Rosny, J. and M. Fink, "Overcoming the diffraction limit in wave physics using a time-reversal mirror and a novel acoustic sink," *Phy. Rev. Lett.*, Vol. 89, 1–4, Sep. 2002.
22. Conti, S. G., P. Roux, and W. A. Kuperman, "Near-field time-reversal amplification," *J. Acoust. Soc. Amer.*, Vol. 121, 3602–3606, Mar. 2007.
23. Lerosey, G., J. de Rosny, A. Tourin, and M. Fink, "Focusing beyong the diffraction limit with far-field time reversal," *Science*, Vol. 315, 1119–1122, Feb. 2007.
24. Rosny, J. D. and M. Fink, "Focusing properties of near-field time reversal," *Phys. Rev. A*, Vol. 92, 1–4, Dec. 2007.
25. Fink, M., "Time-reversal waves and super resolution," *The 4th AIP International Conference and the 1st Congress of the IPIA*, 1–29, 2008.
26. Carminati, R., R. Perrat, J. de Rosny, and M. Fink, "Theory of

the time reversal cavity for electromagnetic fields," *Optics Lett.*, Vol. 32, No. 21, 3107–3109, Nov. 2007.

27. Xiao, S., J. Chen, B.-Z. Wang, and X. Liu, "A numerical study on time-reversal electromagnetic wave for indoor ultra-wideband signal transmission," *Progress In Electromagnetics Research*, Vol. 77, 329–342, 2007.
28. Liu, X., B.-Z. Wang, and L.-W. Li, "Tradeoff of transmitted power in time reversed impulse radio ultra-wideband communications," *IEEE Antenna Wireless Propag. Lett.*, Vol. 8, 1426–1429, 2009.
29. Liu, X., B.-Z. Wang, S. Xiao, and S. Lai, "Post-time-reversed MIMO ultrawideband transmission scheme," *IEEE Trans. Antennas Propag.*, Vol. 58, No. 5, 1731–1738, May 2010.
30. Wang, D., B.-Z. Wang, G.-D. Ge, S.-T. Chen, and M.-C. Tang, "The feasibility of envelope-based time reversal," *Journal of Electromagnetic Waves and Applications*, Vol. 25, No. 1, 63–74, 2011.
31. Ge, G.-D., B.-Z. Wang, H.-Y. Huang, and G. Zheng, "Super-resolution characteristics of time-reversed electromagnetic wave," *Acta. Phys. Sin.*, Vol. 58, No. 12, 8249–8253, Dec. 2009 (in Chinese).
32. Ge, G.-D., B.-Z. Wang, D. Wang, and D. Zhao, "Ultra-wideband communication based on super-resolution characteristics of microstructured array with far-field time-reversal," *Proc. ICIIE*, 264–268, Chengdu, China, Jan. 2011.
33. Carminati, R., M. Nieto-Vesperinas, and J.-J. Greffet, "Reciprocity of evanescent electromagnetic waves," *J. Opt. Soc. Am. A*, Vol. 15. No. 3, 706–712, Mar. 1998.
34. Carminati, R., J. J. Saenz, J.-J. Greffet, and M. Nieto-vesperinas, "Reciprocity, unitarity, and time-reversal symmetry of the S matrix of fields containing evanescent components," *Phys. Rev. A*, Vol. 62, 012712-1–7, 2000.
35. Qu, S. W., C. L. Ruan, B.-Z. Wang, and Q. Xue, "Planar bow-tie antenna embedded in circular aperture within conductive frame," *IEEE Antennas and Wireless Propagation Lett.*, Vol. 5, 399–401, May 2006.